Eur. Phys. J. Special Topics **225**, 699–706 (2016)
© EDP Sciences, Springer-Verlag 2016
DOI: 10.1140/epjst/e2016-60090-2

THE EUROPEAN PHYSICAL JOURNAL SPECIAL TOPICS

Regular Article

Electro-hydrodynamic propulsion of counter-rotating Pickering drops*

P. Dommersnes[a], A. Mikkelsen, and J.O. Fossum

Department of Physics, Norwegian University of Science and Technology, Trondheim, Norway

Received 21 March 2016 / Received in final form 25 May 2016
Published online 15 July 2016

Abstract. Insulating particles or drops suspended in carrier liquids may start to rotate with a constant frequency when subjected to a uniform DC electric field. This is known as the Quincke rotation electro-hydrodynamic instability. A single isolated rotating particle exhibit no translational motion at low Reynolds number, however interacting rotating particles may move relative to one another. Here we present a simple system consisting of two interacting and deformable Quincke rotating particle covered drops, i.e. deformable Pickering drops. The drops attract one another and spontaneously form a counter-rotating pair that exhibits electro-hydrodynamic driven propulsion at low Reynolds number flow.

1 Introduction

Electric fields can induce steady-state hydrodynamic circulation flows in liquids [1,2]. A particular form of such electro-hydrodynamic flow is the Quincke instability, which appears when insulating particles or drops suspended in a carrier liquid are subject to a sufficiently high uniform DC electric field [3,4]. The Quincke rotation instability has these characteristics: The rotation axis is always normal to the applied electric field, the frequency of rotation and the critical electric field is independent of the size of the bead, and the rotation frequency increases with the applied electric field [3,4]. The onset of Quincke rotation in suspensions can lead to several remarkable effects such as effective viscosity reduction [5,6] and increased effective electric conductivity of suspensions [7]. Quincke rotating colloidal particles have been observed to "roll" with a constant velocity on surfaces in liquid crystals and on bubbles [8]. A system of many such interacting self-propelled Quincke rotors has served as a model system for collective swarming motion and active matter [9].

It has also been demonstrated that emulsion drops can undergo Quincke rotation [10–12]. Here we investigate the interaction of two Quincke rotating particle covered drops (i.e. Pickering drops) [13,14] suspended in a bulk liquid, and we find that two such deformable rotors can spontaneously self-organize into a counter-rotating

* Supplementary material in the form of three movies files available from the journal web page at `http://dx.doi.org/10.1140/epjst/e2016-60090-2`

[a] e-mail: `paul.dommersnes@ntnu.no`

pair, and be propelled as the result of their mutual interacting hydrodynamic flow fields. This observation is in agreement with recent models for two-rotor systems of low-Reynolds number swimmers [15,16], and numerical simulations of interacting Quincke rotating particles [17].

2 Electro-hydrodynamic rotation of a single Pickering drop

2.1 Quincke rotation: Background

Quincke rotation of a particle suspended in a liquid is driven by the electric forces acting on the free charges that build up at the surface of a particle [4–6,17]. The instability only occurs if the Maxwell-Wagner electric charge relaxation time of the particle is longer than that of the surrounding fluid, in which case the effective dipole moment of the particle is anti-parallel to the applied electric field. The electric field induces a torque on this dipole, which can create a rotational instability of the particle. Such a steady state rotation of a spherical particle occurs above a critical electric field strength:

$$E_Q = \sqrt{\frac{2\mu\sigma_\ell \left(R+2\right)^2}{3\varepsilon_\ell\varepsilon_p \left(1-RS\right)}} \tag{1}$$

where μ is the viscosity of the suspending liquid, and $R = \frac{\sigma_p}{\sigma_\ell}, S = \frac{\varepsilon_\ell}{\varepsilon_p}$ are dimensionless ratios of electric conductivities, and dielectric constants [4–6,17] . The subscript "p" refers to the particle, and "ℓ" to the suspending liquid. The angular frequency of the Quincke rotation is:

$$\omega = \frac{1}{\tau_{MW}}\sqrt{\frac{E^2}{E_Q^2}-1} \tag{2}$$

where $\tau_{MW} = \frac{\epsilon_p+2\epsilon_\ell}{\sigma_p+2\sigma_\ell}$ is the effective Maxwell-Wagner charge relaxation time of the particle in the liquid [4–6,17]. Notice that Eqs. (1) and (2) are independent of the size of the particle.

2.2 Experiments on Quincke rotation of a single particle laden drop

Our experimental system consists of silicone oil drops suspended in castor oil, and the drops are covered with polyethylene (PE) beads. The electric conductivity of silicone oil is much lower than that of castor oil, and a silicone drop in castor oil may thus Quincke rotate [10,11]. The PE particles have an even lower conductivity than the silicone oil, which will further enhance the charge build-up. We will show in the following that this Pickering drop also exhibit Quincke rotation, however the dynamics can be more complex than that of a solid particle due the deformability of the Pickering particle layer.

The preparation of the Pickering emulsion drops was similar to that of reference [19–21]: Silicone oil (Dow Corning 200/50 cSt, electric conductivity $\sigma_{\rm silc} \sim 0.3\,{\rm pS/m}$, relative permittivity $\varepsilon_{\rm silc} = 2.8$, density $\rho_{\rm silc} = 0.961\,{\rm g/cm^3}$, viscosity $\eta_{\rm silc} = 50\,{\rm cSt}$) was mixed with 50 μm polyethylene (PE) particles (Cospheric LLC with electric conductivity $\sigma_{PE} < 10^{-20}$ S/m, relative permittivity $\varepsilon_{\rm PE} \sim 2.1$, density $\rho_{\rm PE} = 1.0\,{\rm g/cm^3}$). The suspension of PE particles in silicone oil was stirred and ultra-sonicated to avoid particle aggregation. Drops of this suspension were injected by a micropipette into a cell ($15 \times 15 \times 30\,{\rm mm}$) containing Castor oil (Sigma-Aldrich 83912, density of $\rho_{\rm cast} = 0.961\,{\rm g/cm^3}$, electric conductivity $\sigma_{\rm cast} \sim 56\,{\rm pS/m}$, relative

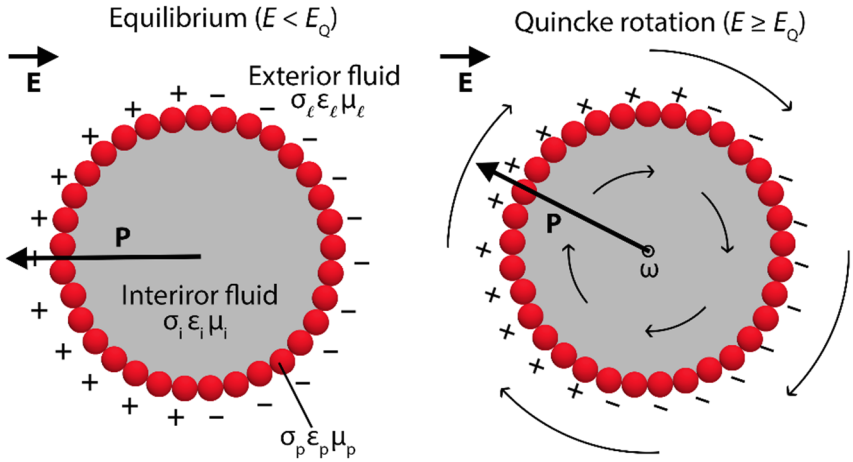

Fig. 1. A sketch illustrating Quincke rotation of a single Pickering emulsion drop covered with electrically insulating particles. (a) The free charge build-up at the surface of the drop results in a dipole moment **P** that is oriented anti-parallel to the direction of the applied electric field. (b) The electric field exerts a torque on the dipole, and above a critical field strength E_Q, the drop starts to rotate at constant frequency. The arrows indicate the direction of the rotation and liquid flow.

permittivity $\varepsilon_{\text{cast}} = 4.7$, viscosity $\eta_{\text{cast}} \sim 1000\,\text{cSt}$). The vertical side walls of the cell consist of two transparent indium tin oxide (ITO) electrodes, in between regular non-conducting glass side-walls. Videos and pictures were recorded using a commercial digital camera mounted on a stereoscope, and the observation view was perpendicular to the applied DC electric field. The PE particles bind irreversibly to the liquid interface due to capillary forces [14,18].

The concentration of PE particles was tuned such that a drop was fully covered when all the beads were at the surface. The experimental critical field for steady Quincke rotation of the Pickering drops was $E_Q \approx 340\,\text{V/mm}$, and the frequency of rotation increases with increasing field strength, in agreement with Eq. (2). Two different modes of rotation is observed, at low fields the Pickering drops rotate like a solid shell (Fig. 2a), at higher fields the particle monolayer goes from a jammed state to a fluid state, with "tank-treading" like dynamics (Fig 2b), reminiscent of tank-treading in fluid bilayer vesicles subject to shear flows [22]. Similar tank-treading like dynamics has also been computed in simulations of particle-laden drops [22]. We observe that larger drops are more prone to electric field induced stretching, resulting in un-jamming of the particle layer and tank-treading like dynamics. For pure drops the electric stretching deformation is proportional to $\frac{a\varepsilon_\ell E^2}{\gamma}$, where a is the radius of the drop, and γ the surface tension [11], which is a result of balance of electric and capillary forces. A similar electro-stretching behavior is expected for Pickering drops studied here, explaining why larger drops exhibit more easily tank-treading. Fig. 2c shows that rotation of solid-shell rotating Pickering drops (Fig. 2a) closely follow the Quincke rotation for solid spherical particles given by Eq. (2). This is not surprising, since a jammed Pickering drop effectively is a solid particle. From the slope in Fig. 2c we obtain an effective Maxwell time $\tau_{MW,exp} \approx 1\,\text{s}$, which is close to the theoretical value $\tau_{MW} = \frac{\epsilon_p + 2\epsilon_\ell}{\sigma_p + 2\sigma_\ell} \approx 0.9\,\text{s}$. To further check our experimental system, we also looked at Quincke rotation of single PE beads of size $100\,\mu\text{m}$ (smallest size for which rotation frequency can be measured by our microscopy). The critical field was found to be $E_Q \approx 400\,\text{V/mm}$, in agreement with the theoretical value given by

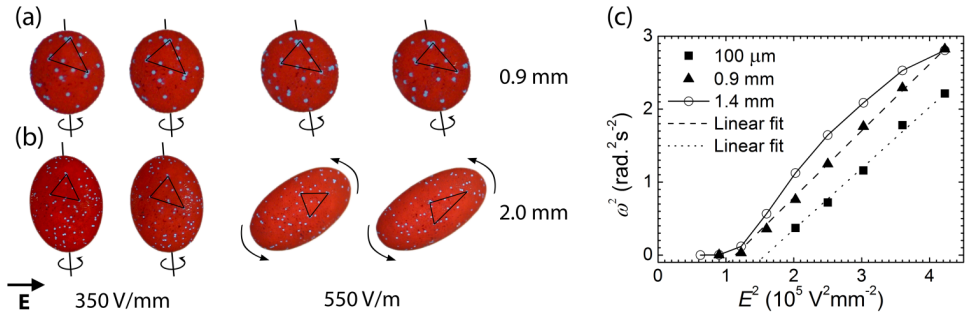

Fig. 2. Pickering silicone drops covered with PE particles (50 μm), and suspended in castor oil. The system was subject to a uniform DC electric field. (a) Quincke rotation of 0.9 mm diameter drops. The electric field strength is initially 350 V/mm (slightly above the critical field needed for Quincke rotation), and was changed to 550 V/mm. The particle layer on the surface of the drop remained jammed (solid layer). The bright particles are differently colored PE particles (50 μm) added to trace the surface flow. (b) Quincke rotation of 2.0 mm diameter drops. The electric field strength was initially 350 V/mm. Upon increasing the field strength to 550 V/mm, the particle layer on the surface of the drop went from solid to fluid, resulting in tank treading like dynamics. (c) Rotation frequency (squared) as a function of field strength (squared) for the solid Pickering drop in (a) (triangles) and a single PE particle of diameter 100 μm (squares). Both follow the Quincke rotation frequency formula given by Eq. (2). The triangles drawn on the Pickering drops in figure (a) and (b) indicate relative positions of tracer particles (PE particles of same size, but different color). (circles) For larger Pickering drops tank-treading occurs even at low fields, and the frequency deviates from the Quincke formula for solid spheres.

Eq. (1). The rotation frequency (squared) was plotted as a function of the square of the applied field (Fig. 2c), and again using the equation for Quincke rotation we obtain an effective Maxwell time $\tau_{MW,exp} = 0.94\,\mathrm{s}$, which also is close to the theoretical value. When the Pickering drop layer goes from solid to liquid, we see deviations from the Quincke rotation formula, leading to more complex dynamics that will be reported in [24].

If the drop is not fully covered, Taylor electrohydrodynamic circulation flows in and around the drop would induce the formation of particle ribbons on the drop surface by convective deposition in the flow field [19–21]. Such flows are not observed around the fully armored drops studied here since the particle layer absorbs the tangential electrostatic stresses.

3 Hydrodynamic propulsion of two interacting Quincke rotors

3.1 Self-propulsion of counter-rotating particles: Theory

Symmetry arguments imply that a single rotating bead cannot swim at low-Reynolds number (unless it interacts with a boundary). However, the combination of two rotors breaks time-invariance symmetry, i.e. reversing the direction of rotation results in a different configuration. Two Quincke rotating spheres interact both via electric dipole-dipole interactions, and hydrodynamic interactions. The general equations describing the motion of two Quincke rotating beads was developed in reference [17], where the authors also found an approximate series expansion solution to the steady state dynamics of co-rotating beads. Here we do a similar series expansion for two counter-rotating beads. The position of sphere 1 and 2 is given by the vectors $\boldsymbol{R}_1$

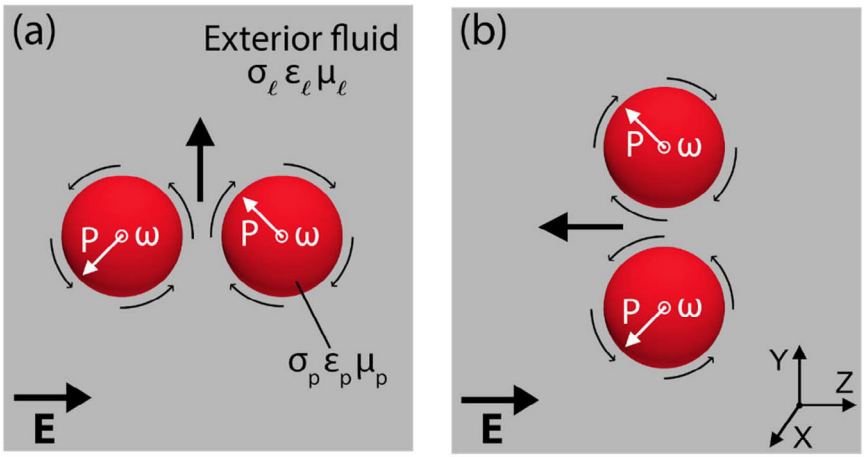

Fig. 3. Two possible relative positions of a pair of Quincke counter-rotating solid spherical particles. (a) The line joining the particles is parallel with the electric field: The direction of hydrodynamic propulsion is perpendicular to the applied electric field. The dipole-dipole interaction is attractive. (b) The line joining particles are perpendicular to the direction of the applied electric field: Hydrodynamic propulsion is in the direction of the field. This situation is unstable since the dipole-dipole force between the two particles is repulsive in this case.

and $\boldsymbol{R}_2$ respectively. The unit vector connecting the beads is: $\widehat{\boldsymbol{R}} = (\boldsymbol{R}_2 - \boldsymbol{R}_1)/R$. The radius of the beads is a. The direction of the dipole of each Quincke rotating sphere is not parallel with the electric field, and the resulting dipole-dipole interaction might be attractive or repulsive depending on the position of the beads, and the direction of these dipoles. The potential energy of a dipole-dipole interaction is: $V = \frac{1}{4\pi\varepsilon_\ell R^3}[\boldsymbol{P}_1 \cdot \boldsymbol{P}_2 - 3(\boldsymbol{P}_1 \cdot \widehat{\boldsymbol{R}})(\boldsymbol{P}_2 \cdot \widehat{\boldsymbol{R}})]$. The direction of the dipoles is determined by the rotation direction of the beads. For two counter-rotating beads, the dipole component perpendicular to the field will be of opposite sign, as indicated in Fig. 3. Consider the dipole-dipole energy for the two simples cases when $\widehat{\boldsymbol{R}}$ is either parallel with the electric field (Fig. 3a) or perpendicular to it (Fig. 3b). The unit vectors in the coordinate systems are $\widehat{\boldsymbol{x}}$, $\widehat{\boldsymbol{y}}$, and $\widehat{\boldsymbol{z}}$ (according to Fig. 3). Consider a case of an applied electric field $\boldsymbol{E}_0 = E_0\widehat{\boldsymbol{z}}$, and the particle rotation angular velocity: $\boldsymbol{\Omega}_1 = \boldsymbol{\Omega}_1\widehat{\boldsymbol{x}}$. When $\widehat{\boldsymbol{R}}$ is either parallel or perpendicular to the applied field, symmetry then implies that: $\boldsymbol{P}_1 \cdot \widehat{\boldsymbol{z}} = \boldsymbol{P}_2 \cdot \widehat{\boldsymbol{z}}$ and $\boldsymbol{P}_1 \cdot \widehat{\boldsymbol{y}} = -\boldsymbol{P}_2 \cdot \widehat{\boldsymbol{y}}$. For the case $\widehat{\boldsymbol{R}}$ is parallel to $\boldsymbol{E}_0$, the interaction potential is therefore always attractive: $V = -\frac{1}{4\pi\varepsilon_\ell R^3}[(\boldsymbol{P}_1 \cdot \widehat{\boldsymbol{y}})^2 + 2(\boldsymbol{P}_1 \cdot \widehat{\boldsymbol{z}})^2]$. For the case $\widehat{\boldsymbol{R}}$ is perpendicular to $\boldsymbol{E}_0$ the potential is always repulsive: $V = \frac{1}{4\pi\varepsilon_\ell R^3}[2(\boldsymbol{P}_1 \cdot \widehat{\boldsymbol{y}})^2 + (\boldsymbol{P}_1 \cdot \widehat{\boldsymbol{z}})^2]$. For other relative positions the dipole-dipole interaction may be either repulsive or attractive, depending on the value of the electric field.

The general electro-hydrodynamic problem of two interacting Quincke rotating solid spheres has been treated in reference [17], the result is a dynamic equation for the dipole moment of sphere 1:

$$\frac{d\boldsymbol{P}_1}{dt} = \boldsymbol{\Omega}_1 \times \left\{ \boldsymbol{P}_1 - 4\pi\varepsilon_\ell a^3 \beta^\infty \left[\boldsymbol{E}_0 - \frac{1}{4\pi\varepsilon_\ell R^3} \boldsymbol{\Pi} \cdot \boldsymbol{P}_2 \right] \right\}$$
$$- \frac{1}{\tau_{MW}} \left\{ \boldsymbol{P}_1 - 4\pi\varepsilon_\ell a^3 \beta^0 \left[\boldsymbol{E}_0 - \frac{1}{4\pi\varepsilon_\ell R^3} \boldsymbol{\Pi} \cdot \boldsymbol{P}_2 \right] \right\} \quad (3)$$

and torque balance on sphere 1:

$$\boldsymbol{\Omega}_1 = \frac{1}{8\pi\mu a^3}\left\{\boldsymbol{P}_1 \times \left[\boldsymbol{E}_0 - \frac{1}{4\pi\varepsilon_\ell R^3}\Pi\cdot\boldsymbol{P}_2\right] - \frac{a^3}{2R^3}\Pi\cdot\left[\boldsymbol{P}_2 \times \left(\boldsymbol{E}_0 - \frac{1}{4\pi\varepsilon_\ell R^3}\Pi\cdot\boldsymbol{P}_1\right)\right]\right\}. \tag{4}$$

Where $\boldsymbol{P}_1$ and $\boldsymbol{\Omega}_1$are the dipole moment and angular velocity respectively, of sphere 1. Similar equations applies for sphere 2. μ is the viscosity of the exterior liquid, the coefficients $\beta^\infty = \frac{\varepsilon_p-\varepsilon_\ell}{\varepsilon_p+2\varepsilon_\ell}$ and $\beta^0 = \frac{\sigma_p-\sigma_\ell}{\sigma_p+2\sigma_\ell}$ are the Clausius-Mossotti factors for spherical particles, and $\Pi = \mathrm{I} - 3\widehat{\boldsymbol{R}}\widehat{\boldsymbol{R}}$. Equations (3) and (4) are valid to order $\frac{1}{R^3}$. Numerical solution of these equations gives quite complex dynamics: in steady state ($\frac{d\boldsymbol{P}_1}{dt} = 0$) the beads may either co-rotate, resulting in orbiting motion, or counter-rotate resulting in propulsion [17]. We find a steady state series expansion solution for counter-rotating beads. The solution for the angular frequency of sphere 1 and 2 can be expressed in a series expansion in $\frac{1}{R}$: $\Omega_1 = -\omega + \frac{c_1}{R^3} + \ldots$and $\Omega_2 = \omega + \frac{c_2}{R^3} + \ldots$, where ω is the rotation frequency of a single isolated bead, given by Eq. (2). The expressions for the coefficients c_1 and c_2 are complicated, however the sum of the two angular frequencies is a simple expression:

$$\Omega_1 + \Omega_2 = \frac{3a^3}{\tau_{MW}R^3}\left(\beta^0 - \beta^\infty\right)\sin(2\theta) \tag{5}$$

where θ is the angle between the applied electric field $\boldsymbol{E}_0$ and the vector $\widehat{\boldsymbol{R}}$ connecting the two beads. This shows that a steady state motion directed along true straight lines require $\widehat{\boldsymbol{R}}$ to be either in perpendicular ($\theta = \frac{\pi}{2}$) or parallel ($\theta = 0$) to the applied electric field. The state perpendicular to the electric field is not stable, since the electric dipoles repel. Therefore, the only steady state propulsion (in straight lines) appears to be when the two beads are aligned with the applied electric field (Fig. 3a), and the beads are propelled perpendicular to the electric field. This is in agreement with simulations of reference [17], which see propulsion perpendicular to the electric field. This does not exclude propulsion at other angles; however, the propulsion is not linear since the beads counter-rotate at slightly different frequencies. In practice this may be a small deviation from straight lines since the difference is of the order $\frac{1}{R^3}$.

The translational speed of two counter-rotating rotors is in the first approximation: $v \approx \frac{T_e}{8\pi\mu R^2}$, where μ is the viscosity of the liquid, R is the distance between the rotors and T_e is the externally applied torque on the rotors [16,17], resulting in approximate propulsion speed: $v \approx \frac{\Omega a^3}{R^2}$. This equation is valid when beads are far apart, however it may give an order of magnitude estimation of the relation between the applied electric torque and the swimming motion for beads that are close. The dipole-dipole interaction in the case Fig. 3a is purely attractive; to obtain a stable counter-rotating pair the attraction must be counter-balanced either by steric (direct contact) or hydrodynamic repulsion due to the rotation.

3.2 Propulsion of counter-rotating Pickering drops: Experiments

We prepared two near identical Pickering drops, as described above, and then initiated counter-rotating Pickering drops by applying an electric field below the Quincke threshold field, thus inducing a simple dipole attraction between the drops. The drops touch, but coalescence is avoided due to the particle armor. The field was subsequently increased above the threshold for Quincke rotation, which resulted in either a stable drop pair, or drop repulsion. For the stable pairs, the drops may either co-rotate or

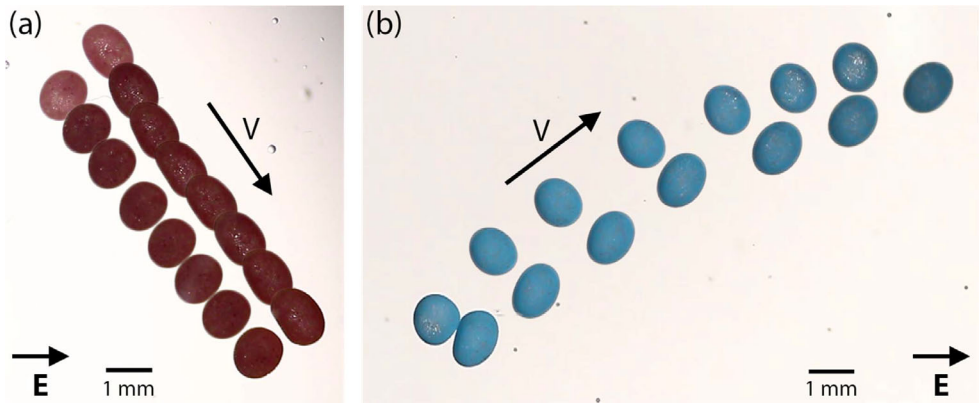

Fig. 4. Cooperative electro-hydrodynamic self-propulsion of a pair of tank-treading particle armored drops. (a) Supporting movie S1: Pickering drops (diameter $\approx$ 1 mm, separation $R \approx 1.3$ mm) covered with 50 μm beads, subject to an electric field of 500 V/mm. The rotational angular velocity of the drops is $\Omega \approx 0.7\,\mathrm{s}^{-1}$, and the experimental propulsion velocity is $v \approx 0.1$ mm/s (b) Supporting movie S2: Pickering drops (diameter $\approx$ 1.0 mm) covered with 30 μm beads, subject to electric field 450 V/mm. The rotational angular velocity of the drops is $\Omega \approx 0.8\,\mathrm{s}^{-1}$, and the experimental propulsion velocity is $v \approx 0.1$ mm/s.

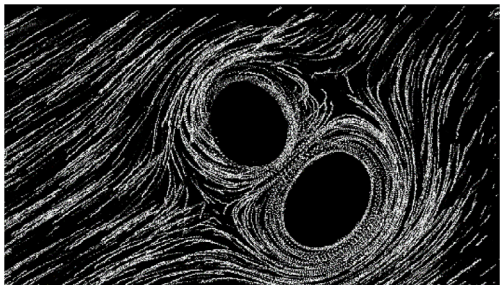

Fig. 5. Experimental hydrodynamic streamlines (tracer particles) around a pair of self-propelled electro-hydrodynamic counter-rotating Pickering drops (diameter $\approx$ 1 mm).

counter-rotate with the rotation axis perpendicular to the electric field, and otherwise it can take any direction in the plane normal to the electric field. This is different from for example magnetic beads in rotating magnetic fields, where all the beads are co-rotating [25]. We observe hydrodynamic (as visualized in Fig. 4 and Fig. 5) propulsion of the two Pickering drops at different angles with the electric field (see supporting material movies S1 and S2), sometimes approximately normal to the field (see supporting material movie S3). We also observe that propulsion along the electric field appears to be unstable in accordance with the discussion above in Sect. 3.1. In all cases the drops are in the tank-treading regime, as described in Fig. 2b. To first order, the propulsion velocity is $v \approx \frac{\Omega a^3}{R^2} \approx \frac{0.7s^{-1}(0.5\,\mathrm{mm})^3}{(1.3\,\mathrm{mm})^2} \approx 0.05$ mm/s, which is close to the experimental propulsion velocity $v \approx 0.1$ mm/s.

We were not able to obtain Quincke rotating pairs of solid PE beads used here, only with tank-treading Pickering drops.

4 Conclusion

We have shown that electro-rotating armored drops may exhibit two dynamic regimes, solid and tank-treading rotation. Two drops may attract one another and form a counter-rotating pair with cooperative hydrodynamic propulsive motion. Future directions may include studies of many self-propelled pairs, for example Pickering emulsions with high density of drops. Future directions might also include propulsion motion using more advanced particle laden drops, such as partly covered drops [26], Janus or patchy shells.

References

1. G.I. Taylor, G.I. Proc. R. Soc. Lond. A **291**, 159 (1966)
2. D.A. Saville, Ann. Rev. Fluid. Mech. **29**, 27 (1997)
3. G. Quincke, Annalen der Physik **295**, 417 (1896)
4. T.B. Jones, IEEE Trans. Ind. Appl. **IA-20**, 845 (1984)
5. L. Lobry, E. Lemaire, J. Electrostat. **47**, 61 (1999)
6. A. Cebers, Phys. Rev. Lett. **92**, 034501 (2004)
7. N. Pannacci, L. Lobry, E. Lemaire, Phys. Rev. Lett. **99**, 094503 (2007)
8. O.D. Lavrentovich, Curr. Opin. Colloid Interface Sci. (2015), `http://dx.doi.org/10.1016/j.cocis.2015.11.008`
9. A. Bricard, J.-B. Caussin, N. Desreumaux, O. Dauchot, D. Bartolo, Nature **503**, 95 (2013)
10. J. Ha, S.M. Yang, Phys. Fluids **12**(4), 764 (2000)
11. H. He, P.F. Salipante, P.M. Vlahovska, Phys. Fluids **25** 032106 (2013)
12. M. Ouriemi, P.M. Vlahovska, Langmuir **31**, 6298 (2015)
13. S.U. Pickering, J. Chem. Soc. **91**, 2001 (1907)
14. R. Aveyard, B.P. Binks, J.H. Clint, Adv. Coll. Int. Sci. **100-102**, 503 (2003)
15. M. Leoni, T.B. Liverpool, EPL **92**, 64004 (2010)
16. Y. Fily, A. Baskaran, M. Cristina Marchetti, Soft Matter. **8**, 3002 (2012)
17. D. Das, D. Saintillan, Phys. Rev. E **87**, 043014 (2013)
18. A.B. Subramaniam, M. Abkarian, H.A. Stone, Nat. Mater. **4**, 553 (2005)
19. Z. Rozynek, A. Mikkelsen, P. Dommersnes, J.O. Fossum, Nat. Commun. **5**, 3945 (2014)
20. P. Dommersnes, Z. Rozynek, A. Mikkelsen, R. Castberg, K. Kjerstad, K. Hersvik, J.O. Fossum, Nat. Commun. **4**, 2066 (2013)
21. Z. Rozynek, P. Dommersnes, A. Mikkelsen, L. Michels, J.O. Fossum, Eur. Phys. J. Special Topics **223**, 1859 (2014)
22. V. Kantsler, V. Steinberg, Phys. Rev. Lett. **95**, 258101 (2005)
23. S. Frijters, F. Gunther, J. Harting, Soft Matter. **8**, 6542 (2012)
24. A. Mikkelsen, Z. Rozynek, A. Gholamipour-Shirazi, P. Dommersnes, M.S. Carvalho, J.O. Fossum (preprint).
25. G. Helgesen, P. Pieranski, A.T. Skjeltorp, Phys. Rev. Lett. **64**, 1425 (1990)
26. P. Dommersnes, J.O. Fossum, Eur. Phys. J. Special Topics **225**(4), 699 (2016)